

Published in final edited form as:

Biochem Biophys Res Commun. 2011 August 26; 412(2): 220–225. doi:10.1016/j.bbrc.2011.07.063.

Plasmalemmal vesicle associated protein (PV1) modulates SV40 virus infectivity in CV-1 cells

Dan Tse¹, David A. Armstrong¹, Ariella Oppenheim⁵, Dimitry Kuksin⁴, Leonard Norkin⁴, and Radu V. Stan^{1,2,3,6}

¹Department of Pathology, Dartmouth Medical School, Lebanon, NH

²Departments of Microbiology and Immunology, Dartmouth Medical School, Lebanon, NH

³Heart and Vascular Research Center, Dartmouth Medical School, Lebanon, NH

⁴Department of Microbiology, University of Massachusetts, Amherst, MA

⁵Department of Hematology, Hadassah Medical School, Jerusalem, Israel

Abstract

Plasmalemmal vesicle associated protein (Plvap/PV1) is a structural protein required for the formation of the stomatal diaphragms of caveolae. Caveolae are plasma membrane invaginations that were implicated in SV40 virus entry in primate cells. Here we show that de novo Plvap/PV1 expression in CV-1 green monkey epithelial cells significantly reduces the ability of SV40 virus to establish productive infection, when cells are incubated with low concentrations of the virus. However, in presence of high viral titers PV1 has no effect on SV40 virus infectivity. Mechanistically, PV1 expression does not reduce the cell surface expression of known SV40 receptors such as GM1 ganglioside and MHC class I proteins. Furthermore, PV1 does not reduce the binding of virus-like particles made by SV40 VP1 protein to the CV-1 cell surface and does not impact their internalization when cells are incubated with either high or low VLP concentrations. These results suggest that PV1 protein is able to block SV40 infectivity at low but not at high viral concentration either by interfering with the infective internalization pathway at the cell surface or at a post internalization step.

1. Introduction

Caveolae are invaginations of plasma membrane of regular shape and size, which occur in most mammalian cell types. Caveolae were implicated in cell biological processes such as mechanotransduction, endocytosis, pathogen uptake and infectivity, cholesterol transport and efflux, signaling (*i.e.* mechanosensing, nitric oxide, growth factors and integrins) and cell migration. Due to these multiple roles, caveolae are important for mammalian physiology regulating multiple aspects of the cardiovascular function, adipogenesis, immune function as well as glucose, cholesterol and lipoprotein metabolism [1; 2; 3].

© 2011 Elsevier Inc. All rights reserved.

⁶Contact: Radu V. Stan, M.D., Department of Pathology, Dartmouth Medical School, One Medical Center Drive, Lebanon, NH 03756. Tel: (603) 650-8781, Fax: (603) 650-6120, Radu.V.Stan@Dartmouth.edu.

Publisher's Disclaimer: This is a PDF file of an unedited manuscript that has been accepted for publication. As a service to our customers we are providing this early version of the manuscript. The manuscript will undergo copyediting, typesetting, and review of the resulting proof before it is published in its final citable form. Please note that during the production process errors may be discovered which could affect the content, and all legal disclaimers that apply to the journal pertain.

In select endothelial cells, caveolae are provided with a stomatal diaphragm (SD) [4], a thin (~5–7nm) protein structure that occurs in caveolae necks [5; 6]. PV1, a vertebrate protein encoded by the *Plvap* gene [5; 7], was shown to be restricted to the SDs of caveolae [4] as well as the diaphragms of fenestrae and transendothelial channels, cellular structures implicated in vascular permeability [8; 9; 10]. Based on data obtained in cells in culture [8], PV1 was proposed to function as a key structural component of the diaphragms [5; 6].

There is no clear function assigned to caveolae SDs. The location of the SDs in caveolae necks and their “barrier-like” appearance led us to the hypothesis that they could affect caveolae-mediated uptake of cargo. Caveolae undergo endocytosis although there is no specific cargo of caveolae endocytosis described to date [11]. One of the most studied caveolar cargoes is the SV40 virus [12; 13; 14], a non-enveloped double stranded DNA virus of the polyomavirus family, which replicates in the cell nucleus [15; 16]. The main structural components of SV40 are 72 homopentamers of the major capsid protein, VP1, icosahedrally arranged [16; 17]. SV40 uses MHC class I molecules [18; 19; 20; 21; 22] and GM1 ganglioside [12; 14; 23; 24; 25; 26] as receptors. Although SV40 viruses enter cells via multiple endocytic mechanisms [15] the caveolae/lipid raft pathways are the only important pathways for establishment of productive infection [16; 23; 24]. Indeed, SV40 is internalized in caveolin-1 containing vesicles [12; 25]. However, especially at high SV40 concentrations, the virus induces membrane invaginations devoid of caveolin-1, which mediate its internalization and productive infection [24].

Here, we report that de novo expression of PV1 and formation of the SD of caveolae in CV-1 monkey epithelial cells, blocks the infectivity of SV40 virus when cells were incubated with low viral titers whereas at high viral titers, PV1 expression has no effect.

2. Materials and Methods

2.1 Materials

Bovine serum albumin (BSA) were from Sigma Chemical Co (St. Louis, MO); DMEM (Dulbecco's modified Eagle medium), antibiotics, Alexa dye protein labeling kits from Invitrogen (Carlsbad, CA), fetal bovine serum (FBS) from Atlanta Biologicals (Norcross, GA) (San Diego, CA). were from Pierce (Rockford, IL). All the other materials were either from Thermo Fisher (Pittsburgh, PA) or Sigma, as reported in our previous papers.

2.2 Cells

CV-1 African green monkey kidney cells and HeLa cells were purchased from the American Type Tissue Culture Association (Rockville, MD) and maintained in DMEM containing 10% FBS, 100 units/ml penicillin, 100 µg/ml streptomycin, and 50 µg/ml gentamycin (Invitrogen, Carlsbad, CA). Cells were cultured at 37°C under a 5% CO₂ atmosphere. The hybridoma secreting the mouse anti-human PV1 IgG2a mAb PAL-E [27] was a gift from Dr. M.L. Kahn, U. Pennsylvania. The hybridoma secreting the anti-VP1 monoclonal antibody, clone PAb 597 was previously described [28].

2.3 Antibodies

The rabbit anti-caveolin 1 pAb was from BD Pharmingen (San Diego, CA) and mouse anti-HA mAb clone HA.11 was from Santa Cruz (Santa Cruz, CA). Affinity purified mouse anti-human PV1 mAb PAL-E was obtained either from Abcam (Cambridge, MA) or affinity purified on a Protein G column from PAL-E hybridoma supernatant. Chicken anti-human PV1C pAb used for blotting was previously described [8]. Mouse anti-human PV1 mAb clone PAL-E and mouse anti-VP1 clone PAb597 were produced by BioXCell (Lebanon, NH). The unlabeled and HRP-conjugated rabbit anti-chicken IgY and the goat anti-mouse

IgG-HRP were from Biodesign (Kennebunk, ME). Goat anti-mouse IgG-Alexa568 F(ab)₂ reporter antibody was from Invitrogen (Carlsbad, CA). Mouse anti-human PV-1 mAb PAL-E as well as mouse anti-VP1 clone PAb 597 were labeled with Alexa (488, 568 or 647) fluorophores (Invitrogen), as per manufacturer's instructions.

2.4 Constructs and Viruses

The hPV1-3xHA-IRES-hrGFP bicistronic construct that also encoded for humanized *Renilla* green fluorescent protein (hrGFP) was reported before [8]. SV40 virus stocks were prepared from CV-1 cell culture supernatants as described [17].

2.5 Transfection of CV-1 cells with PV1HA and infection with SV40 virus

Human PV1HA was expressed in CV-1 cells by transfection of PV1HA-IRES-hrGFP using Fugene 6 (Roche). Control cells were either mock-transfected (no DNA included) or empty vector transfected (EV). The hrGFP expressing cells were flow sorted using a FACSaria cytometer (BD Biosciences) and plated at 60% density in 8 well Permax chamber slides (Nunc). The cells were allowed to attach and spread for 8h when they were chilled to 4°C and then incubated (30 min, 4°C) with SV40 virus-containing growth medium (DMEM containing 10% FBS) to allow the virus to bind to its cell surface receptors. The unbound virus was washed away at 4°C after which the cells were warmed to 37°C and incubated (24h) in growth medium to allow the virus to enter the cells and establish productive infection.

Infected cells were identified by indirect immunofluorescent staining using monoclonal antibodies against VP1, the major SV40 capsid protein. Briefly, the cells were rinsed (3×2min) in PBS, fixed (10min, -20°C) in methanol, rinsed again (3×2min) in PBS, blocked (1h, RT) in 10% goat serum in PBS, incubated (1h, 37°C) with anti-VP1 hybridoma supernatant, rinsed (6×3min) in PBS, incubated (30min, RT) with a goat anti-mouse IgG-Alexa 568 F(ab)₂, rinsed (6×3min) in PBS, stained with 4',6-diamidino-2-phenylindole, dihydrochloride (DAPI) and mounted (PermaFluor) for laser confocal fluorescence microscopy. Infected cells displayed intense nuclear staining [17].

2.6 Immunofluorescence to detect cell surface PV1HA

To determine cell surface expression of PV1HA, 24 hours post transfection live cells were labeled (30min, 10°C) with anti-PV1-Alexa647 mAb diluted in growth medium, rinsed (6×3min, 4°C) in ice-cold PBS, fixed (10min, RT) in 2% paraformaldehyde in PBS, rinsed again (6×3min, 4°C) in PBS, incubated (10min, RT) in PBS containing DAPI and mounted in PermaFluor (Thermo Fisher). In separate experiments, cells were first fixed (10min, RT) in 2% paraformaldehyde in PBS, rinsed in PBS, blocked (1h, RT) in 10% goat serum in PBS, labeled (2h, RT) with anti-HA mAbs diluted in 10% goat serum in PBS, rinsed and labeled (30min, RT) with fluorescent reporter goat anti-mouse IgG-Alexa 647 F(ab)₂ fragments (Invitrogen), rinsed again (6×3min, RT) with PBS and mounted in PermaFluor.

2.7 Laser confocal microscopy

Labeled cells were imaged by laser confocal fluorescence microscopy using a Zeiss 510 Meta System (Zeiss) using 20× or 60× objectives and appropriate laser excitation. Image processing was done in ImageJ.

2.8 Cell fractionation and Western blotting

Transfected CV-1 cells were homogenized and total cellular membranes were obtained as before [8]. The membrane pellet was solubilized (10mM Tris, pH 6.8, 0.5%SDS, protease inhibitors (Sigma)). The protein content of different fractions was determined by the

bicinchoninic acid method (Pierce) using BSA standards made in solubilization buffer. Equal amounts of membrane proteins (20 μ g) were resolved by 8% SDS-PAGE, transferred to PVDF membrane and probed by immunoblotting with various antibodies. ECL was used as a detection system and images acquired using a G:Box Chemi XT16 system and GeneSnap software (Syngene).

2.9 Flow Cytometry

To detect cell surface expression of PV1HA, GM1 and MHC class I, CV-1 cells were detached (10min, 37°C) using the Cell Dissociation Solution (Sigma), resuspended in 1% BSA in PBS and incubated (30min, on ice) with anti-PV1, CTxB–Alexa647 or anti-MHC I, respectively. Cells were rinsed and analyzed by either using a CANTO flow cytometer controlled by DIVA software (BD Biosciences). Data analysis was carried out using FlowJo version 9.3 (Tree Star, Ashland, OR) software. Each experiment had 4–8 samples per time point and was repeated at least three times. Statistical significance was calculated using Student's *t* test.

2.10 VP1-VLP production, labeling, binding and internalization

Recombinant baculovirus expressing VP1 (SwissProt P03087) from the polyhedrin promoter was used for production of virus-like particles (VLPs) as previously described [29]. VLPs were labeled with Alexa dyes (Invitrogen) and the unbound dye was removed by size exclusion chromatography with Nap-5 columns (GE Healthcare). The integrity of labeled VLPs was determined by whole mount fluorescence and dynamic light scattering (Zetasizer, Malvern).

To measure VLP binding, live transfected CV-1 cells were labeled (30min, 4°C) while adherent with fluorescent VLPs in growth medium, rinsed in PBS to remove unbound VLP, detached non-enzymatically with cell dissociation solution (Sigma) and examined by flow cytometry.

For VLP internalization, after VLP binding transfected cells shifted to 37°C for 15 or 120 minutes, the cells were acid washed, detached in a mixture of trypsin/EDTA and examined by flow cytometry.

3. Results

3.1. De novo expression of PV1 reduces SV40 infectivity at low but not high viral doses

Caveolae uptake of SV40 virus has a role in establishing a productive viral infection in CV-1 monkey epithelial cells [15; 30]. CV-1 cells do not express PV1 and, by electron microscopy lack the SDs of caveolae, making them ideal for experiments to test whether the formation of SDs blocks SV40 infectivity.

HA epitope-tagged human PV1 (PV1-HA) was expressed in CV-1 cells using a bicistronic vector that also encoded for humanized *Renilla* green fluorescent protein (hrGFP), previously characterized [8]. We used a validated construct encoding for human PV1, which has high homology to primate PV1 (>90% identity and >95% similarity) (Fig 1). The expression of PV1-HA was checked by immunoblotting (Fig 2A) whereas the correct targeting of human PV1 to the cell surface in CV-1 cells was ascertained by immunofluorescence of unpermeabilized live cells (Fig 2B) or by flow cytometry (Fig 2C) with anti-HA or PV1 antibodies, respectively. As shown in Fig 2C, there was an excellent correlation between hrGFP expressing cells and surface PV1 expression.

In order to obtain quantitative data on the effect of PV1 on SV40 infectivity, we have used a protocol detailed in Figure 3A. By this the PV1-HA or empty vector transiently transfected cells were sorted by flow cytometry using hrGFP fluorescence, ten hours post transfection. An example of the gating used is shown in Fig 3B. The sorted cells were plated at ~60% density on 8 well chamber slides and allowed to attach for 8–12 more hours, until the cells were well spread. Upon visual confirmation of cell spreading, the cells were incubated with SV40 virus for 30min at 10°C in order for the virus to bind to the cell surface receptors. Upon washing the non-bound excess SV40, the bound virus was allowed to enter the hrGFP-sorted cells and to establish productive infection. The number of virus particles used yielded a multiplicity of infection (MOI) of approximately 0.5 (i.e. half of the cells present in the well were infected). Viral replication in the nucleus was detected as intense nuclear staining using an anti-VP1 capsid protein mAb [17]. By this measure, the expression of PV1 in CV-1 cells led to a dramatic decrease of SV40 infectivity, as shown in Fig 3C and 3D.

Consequent to recent reports [24] showing that SV40 virus can induce its own carriers at high MOI(>200), we tested whether PV1 has the ability to block SV40 infectivity in presence of high viral concentrations. As shown in Figs 3E and 3F, expression of PV1 has no effect on SV40 infectivity at high viral doses.

3.2. Expression of PV1 does not modify cell surface expression levels of SV40 receptors

In order to gain mechanistic insight into how PV1 might reduce SV40 infectivity, we have determined the cell surface levels of known SV40 receptors, such as GM1 ganglioside and MHC class I molecules. MHC class I molecules were detected with an anti HLA antibody known to react with simian MHC class I.

To exclude a possible downregulation of the surface amounts of the receptors being a cause for decreased SV40 infectivity, we have quantified the cell surface expression of GM1 ganglioside and MHC class I molecules by immunofluorescence (not shown) and flow cytometry using fluorescently labeled cholera toxin B subunit (Fig 4A) and anti-MHC class I antibody (Fig 4B), respectively. For this we have used PV1-HA and hrGFP transiently transfected CV-1 cell, which were labeled either adherent or in suspension. PV1 expression did not decrease the surface expression of either GM1 (Fig 4A and C) or MHC class I (Fig 4A and B) molecules, ruling out a role for receptor down regulation.

3.3. Expression of PV1 does not modify the binding of VP1 virus-like particles

To further probe the cause of decreased infectivity of SV40 virus we have employed Alexa 647 dye labeled virus-like particles made of VP1 capsid protein [24]. The VLPs were used as surrogates for SV40 virus to test the binding and internalization. As shown in Fig 4D, PV1 expression does not impact the binding of VLPs to CV-1 cells. PV1 expression also does not seem to impact the internalization of VLPs (Fig 4E) at either 15 or 120 minutes post VLP binding at either low (1) or high (200) viral particles per cell, concentration.

4. Discussion

The work presented in here stems from our long time interest in determining the function of caveolae and their SDs, which is currently unknown. Although, caveolae have been involved in a plethora of cellular functions, to date there is no specific assay for caveolar function, significantly hampering the task of determining the role of the SD.

Early morphological data have suggested that the SDs might play a barrier role, as they seem to oppose the access of cargo such as cationized ferritin [31] or albumin[32] to the lumen of caveolae, whereas allowing the access of HRP. Thus, the SDs might modulate

caveolae endocytosis, thought to mediate the uptake of cargoes such as serum albumin [33; 34], integrins [35], toxins (i.e. cholera toxin) or viruses (i.e. polyoma viruses such as SV40).

SV40 virus binds to cell surface receptors such as GM1 ganglioside [24] and MHC class I molecules [19] from where, the virus translocates to preformed membrane invaginations such as those of the caveolae/lipid raft pathway which mediate its internalization. At high concentrations, by clustering GM1 the virus induces the formation of tubular invaginations, which will mediate the virus internalization in caveolae independent manner [24]. Both pathways converge into the same endosomes from where the virus journeys to the endoplasmic reticulum, cytoplasm and the nucleus where it will replicate (establishing a so-called productive infection). Both lipid raft containing endocytosis pathways (i.e. caveolae dependent and independent) have been demonstrated to be essential for viral penetration and establishment of productive infection. To note, the virus is able to enter mammalian cells via other uptake pathways, but these pathways do not result in productive infection. Thus, SV40 infectivity at low viral concentrations is a good test for whether the caveolae SDs have any impact on viral entry via caveolae.

De novo expression of PV1 has been shown to induce the formation of caveolae SDs in endothelial cells and fibroblasts in culture. Taking advantage of PV1 ability to induce SD formation, we have expressed it in CV-1 cells, and asked whether it has an effect on SV40 infectivity. Indeed, our data clearly show that expression of PV1 in CV-1 cells significantly reduces SV40 infectivity at low viral concentrations, whereas it does not have an effect at high viral doses. Unfortunately, we could not do these experiments in endothelial cells, the only cell type known to express PV1 and SDs physiologically. While SV40 is able to enter endothelial cells with very low efficiency due to low levels of GM1 expression in these cells, this rarely, if ever, results in productive infection (our unpublished data).

Mechanistically, we were able to rule out the down regulation of cell surface receptors such as GM1 and MHC class I upon PV1 expression, to be responsible for decreased infectivity. Moreover, PV1 expression did not reduce the binding of fluorescent VP1 VLP (a non-infectious SV40 surrogate) to the cell surface, bringing further support to this idea. Interestingly, PV1 did not reduce the internalization of fluorescent VP1 VLP at either low or high dose. However, testing the internalization of VLPs by our flow cytometry assay proved to be challenging due to high avidity of the pentavalent VLPs for their cell surface receptors precluding reliable removal of the non-internalized surface bound VLPs.

These data suggest that either PV1 is by blocking a minor pathway that cannot be easily detected by the flow cytometry assay we have employed or PV1 acts at a latter time in the infective pathway.

In summary we have found conditions by which SV40 infectivity can be drastically reduced in conditions of low viral concentration. These data are significant as the low viral concentration is a norm for initial infection.

Highlights

- Expression of PV1 in Cv-1 cells reduces SV40 virus infectivity at low viral titer
- PV1 expression does not reduce the cell surface levels of SV40 receptors GM1 ganglioside and MHC class I molecules
- PV1 expression does not inhibit binding and internalization of SV40 VP-1 virus like particles

Acknowledgments

This work has been supported from the NIH grants HL65418, HL83249 and HL92085 to RVS. We would like to thank M. Abd-El-Latif for the preparation of VLPs and D. Madden and N. Shworak for discussions on the manuscript.

References

1. Bastiani M, Parton RG. Caveolae at a glance. *J Cell Sci.* 2010; 123:3831–3836. [PubMed: 21048159]
2. Hansen CG, Nichols BJ. Exploring the caves: caveins, caveolins and caveolae. *Trends Cell Biol.* 2010; 20:177–186. [PubMed: 20153650]
3. Lajoie P, Nabi IR. Lipid rafts, caveolae, and their endocytosis. *Int Rev Cell Mol Biol.* 2010; 282:135–163. [PubMed: 20630468]
4. Stan RV, Ghitescu L, Jacobson BS, Palade GE. Isolation, cloning, and localization of rat PV-1, a novel endothelial caveolar protein. *J Cell Biol.* 1999; 145:1189–1198. [PubMed: 10366592]
5. Stan RV. Endothelial stomatal and fenestral diaphragms in normal vessels and angiogenesis. *J Cell Mol Med.* 2007; 11:621–643. [PubMed: 17760829]
6. Tse D, Stan RV. Morphological heterogeneity of endothelium. *Semin Thromb Hemost.* 2010; 36:236–245. [PubMed: 20490976]
7. Stan RV, Arden KC, Palade GE. cDNA and protein sequence, genomic organization, and analysis of cis regulatory elements of mouse and human PLVAP genes. *Genomics.* 2001; 72:304–313. [PubMed: 11401446]
8. Stan RV, Tkachenko E, Niesman IR. PV1 is a key structural component for the formation of the stomatal and fenestral diaphragms. *Mol Biol Cell.* 2004; 15:3615–3630. [PubMed: 15155804]
9. Stan RV, Kubitzka M, Palade GE. PV-1 is a component of the fenestral and stomatal diaphragms in fenestrated endothelia. *Proc Natl Acad Sci U S A.* 1999; 96:13203–13207. [PubMed: 10557298]
10. Ioannidou S, Deinhardt K, Miotla J, Bradley J, Cheung E, Samuelsson S, Ng YS, Shima DT. An in vitro assay reveals a role for the diaphragm protein PV-1 in endothelial fenestra morphogenesis. *Proc Natl Acad Sci U S A.* 2006; 103:16770–16775. [PubMed: 17075074]
11. Parton RG, Simons K. The multiple faces of caveolae. *Nat Rev Mol Cell Biol.* 2007; 8:185–194. [PubMed: 17318224]
12. Pelkmans L, Kartenbeck J, Helenius A. Caveolar endocytosis of simian virus 40 reveals a new two-step vesicular-transport pathway to the ER. *Nat Cell Biol.* 2001; 3:473–483. [PubMed: 11331875]
13. Tagawa A, Mezzacasa A, Hayer A, Longatti A, Pelkmans L, Helenius A. Assembly and trafficking of caveolar domains in the cell: caveolae as stable, cargo-triggered, vesicular transporters. *J Cell Biol.* 2005; 170:769–779. [PubMed: 16129785]
14. Singh RD, Holicky EL, Cheng ZJ, Kim SY, Wheatley CL, Marks DL, Bittman R, Pagano RE. Inhibition of caveolar uptake, SV40 infection, and beta1-integrin signaling by a nonnatural glycosphingolipid stereoisomer. *J Cell Biol.* 2007; 176:895–901. [PubMed: 17371832]
15. Marsh M, Helenius A. Virus entry: open sesame. *Cell.* 2006; 124:729–740. [PubMed: 16497584]
16. Mercer J, Schelhaas M, Helenius A. Virus entry by endocytosis. *Annu Rev Biochem.* 2010; 79:803–833. [PubMed: 20196649]
17. Norkin LC. Simian virus 40 infection via MHC class I molecules and caveolae. *Immunol Rev.* 1999; 168:13–22. [PubMed: 10399061]
18. Anderson HA, Chen Y, Norkin LC. Bound simian virus 40 translocates to caveolin-enriched membrane domains, and its entry is inhibited by drugs that selectively disrupt caveolae. *Mol Biol Cell.* 1996; 7:1825–1834. [PubMed: 8930903]
19. Anderson HA, Chen Y, Norkin LC. MHC class I molecules are enriched in caveolae but do not enter with simian virus 40. *J Gen Virol.* 1998; 79(Pt 6):1469–1477. [PubMed: 9634090]
20. Chen Y, Norkin LC. Extracellular simian virus 40 transmits a signal that promotes virus enclosure within caveolae. *Exp Cell Res.* 1999; 246:83–90. [PubMed: 9882517]

21. Parton RG, Lindsay M. Exploitation of major histocompatibility complex class I molecules and caveolae by simian virus 40. *Immunol Rev.* 1999; 168:23–31. [PubMed: 10399062]
22. Stang E, Kartenbeck J, Parton RG. Major histocompatibility complex class I molecules mediate association of SV40 with caveolae. *Mol Biol Cell.* 1997; 8:47–57. [PubMed: 9017594]
23. Damm EM, Pelkmans L, Kartenbeck J, Mezzacasa A, Kurzchalia T, Helenius A. Clathrin- and caveolin-1-independent endocytosis: entry of simian virus 40 into cells devoid of caveolae. *J Cell Biol.* 2005; 168:477–488. [PubMed: 15668298]
24. Ewers H, Romer W, Smith AE, Bacia K, Dmitrieff S, Chai W, Mancini R, Kartenbeck J, Chambon V, Berland L, Oppenheim A, Schwarzmann G, Feizi T, Schwille P, Sens P, Helenius A, Johannes L. GM1 structure determines SV40-induced membrane invagination and infection. *Nat Cell Biol.* 2010; 12(11–8; sup):1–12.
25. Pelkmans L, Puntener D, Helenius A. Local actin polymerization and dynamin recruitment in SV40-induced internalization of caveolae. *Science.* 2002; 296:535–539. [PubMed: 11964480]
26. Richards AA, Stang E, Pepperkok R, Parton RG. Inhibitors of COP-mediated transport and cholera toxin action inhibit simian virus 40 infection. *Mol Biol Cell.* 2002; 13:1750–1764. [PubMed: 12006667]
27. Keuschnigg J, Henttinen T, Auvinen K, Karikoski M, Salmi M, Jalkanen S. The prototype endothelial marker PAL-E is a leukocyte trafficking molecule. *Blood.* 2009; 114:478–484. [PubMed: 19420356]
28. Norkin LC, Kuksin D. The caveolae-mediated sv40 entry pathway bypasses the golgi complex en route to the endoplasmic reticulum. *Virology.* 2005; 2:38. [PubMed: 15840166]
29. Butin-Israeli V, Drayman N, Oppenheim A. Simian virus 40 infection triggers a balanced network that includes apoptotic, survival, and stress pathways. *J Virol.* 2010; 84:3431–3442. [PubMed: 20089643]
30. Norkin LC. Caveolae in the uptake and targeting of infectious agents and secreted toxins. *Adv Drug Deliv Rev.* 2001; 49:301–315. [PubMed: 11551401]
31. Clementi F, Palade GE. Intestinal capillaries. I. Permeability to peroxidase and ferritin. *J Cell Biol.* 1969; 41:33–58. [PubMed: 5775791]
32. Villaschi S, Johns L, Cirigliano M, Pietra GG. Binding and uptake of native and glycosylated albumin-gold complexes in perfused rat lungs. *Microvasc Res.* 1986; 32:190–199. [PubMed: 3762426]
33. Milici AJ, Watrous NE, Stukenbrok H, Palade GE. Transcytosis of albumin in capillary endothelium. *J Cell Biol.* 1987; 105:2603–2612. [PubMed: 3320050]
34. Schnitzer JE, Oh P. Albondin-mediated capillary permeability to albumin. Differential role of receptors in endothelial transcytosis and endocytosis of native and modified albumins. *J Biol Chem.* 1994; 269:6072–6082. [PubMed: 8119952]
35. Sharma DK, Brown JC, Cheng Z, Holicky EL, Marks DL, Pagano RE. The glycosphingolipid, lactosylceramide, regulates beta1-integrin clustering and endocytosis. *Cancer Res.* 2005; 65:8233–8241. [PubMed: 16166299]

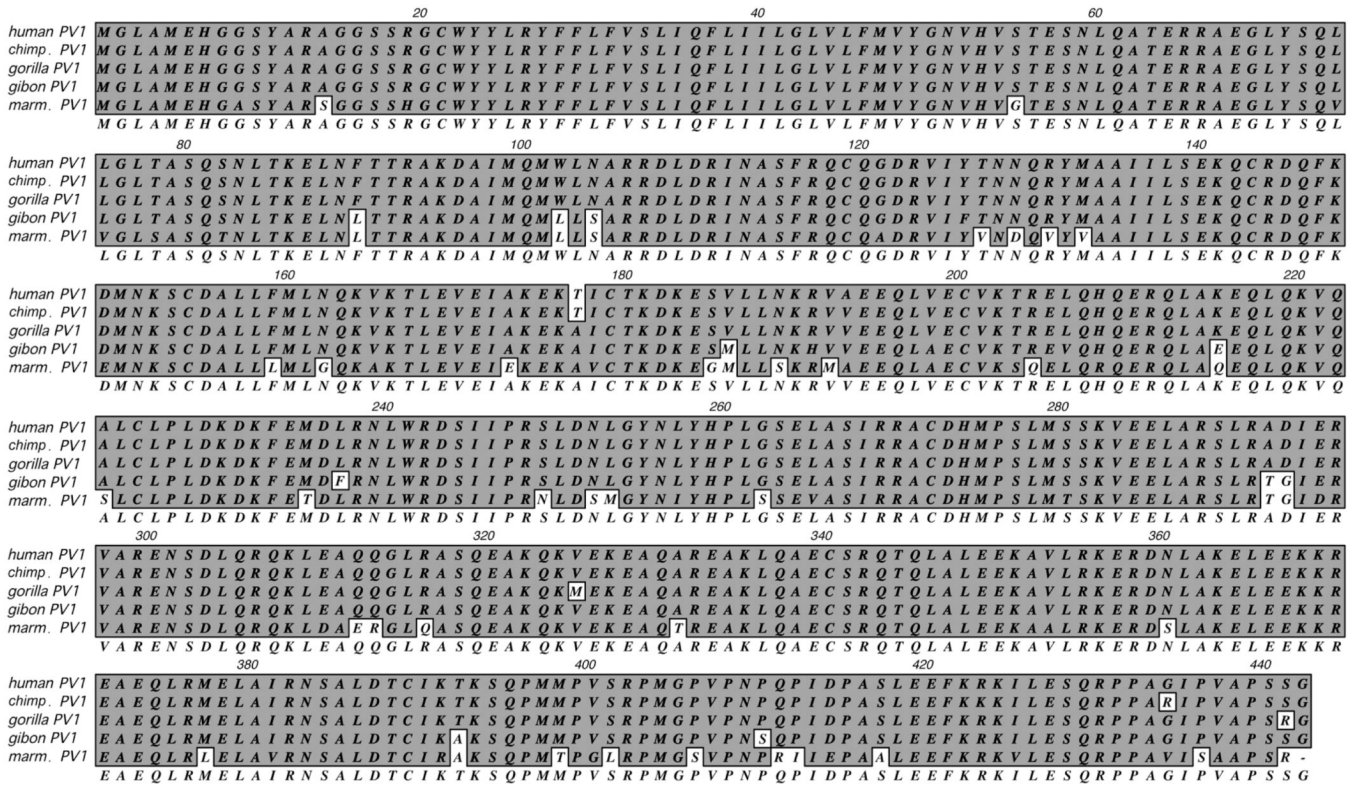


Figure 1. ClustalW alignment of human and primate PV1 protein sequences demonstrating the high degree of homology between the species.

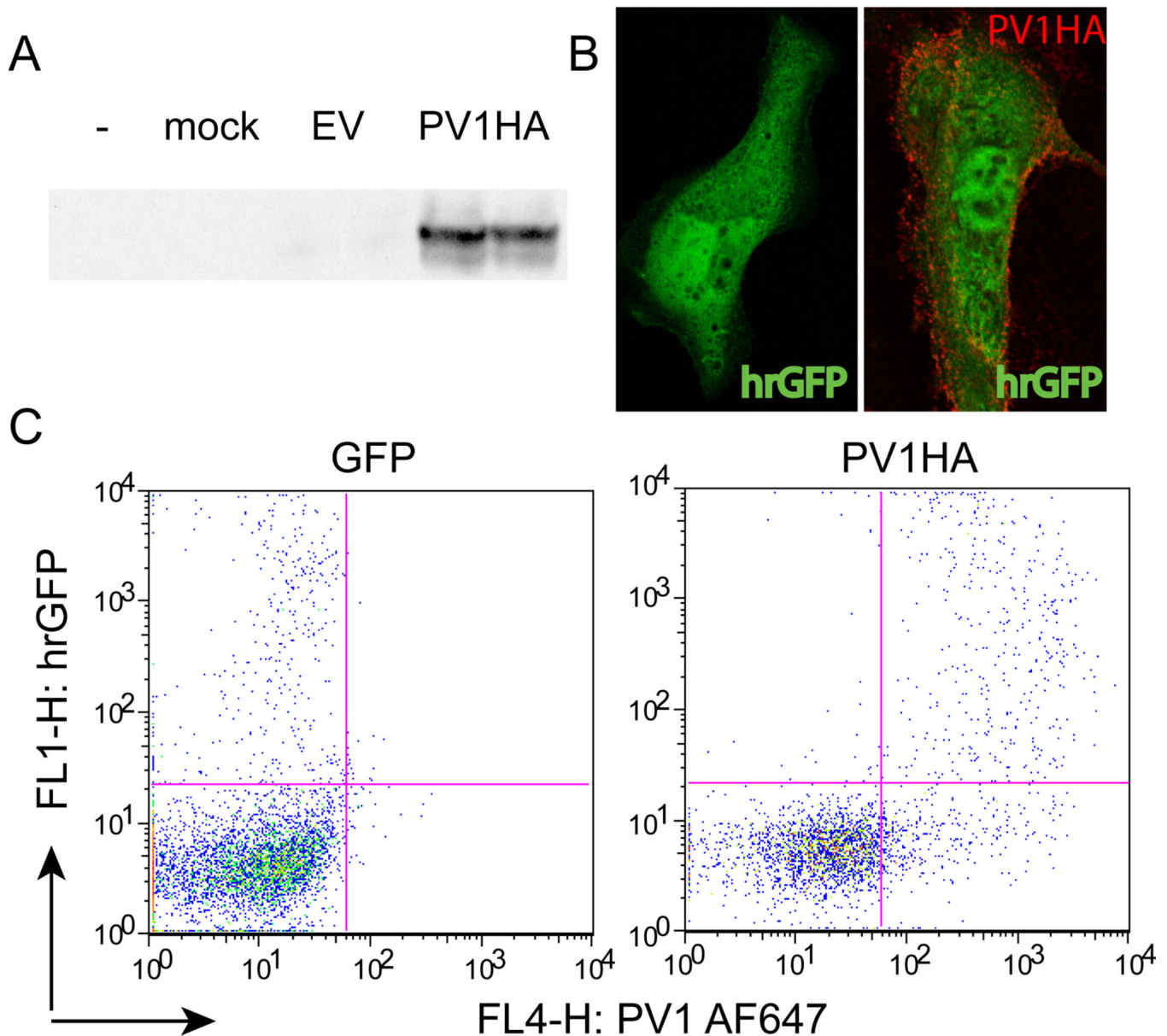


Figure 2. PV1HA is expressed at the cell surface in CV-1 cells

A) Western blotting with anti-HA antibodies of lysates from nontransfected (-), mock (mock), hrGFP and PV1HA-IRES-hrGFP (PV1HA) transfected CV-1 cells. Only PV1HA transfected cells demonstrate bands of an appropriate size. B) Confocal microscopy of anti-HA mAb labeled nonpermeabilized CV-1 cells transfected with either hrGFP (*left*) or PV1HA-IRES-hrGFP (*right*) constructs demonstrating a characteristic cell surface punctate staining only in PV1HA expressing cells. The images represent the maximum intensity projection of stacks made of several confocal slices. C) Flow cytometry with anti-PV1 antibodies directly coupled to Alexa 647 demonstrating cell surface staining only in PV1HA expressing cells (*right*) and no staining in hrGFP transfected cells (*left*). To note, in PV1HA-IRES-hrGFP transfected cells, all hrGFP positive cells are also PV1 positive.

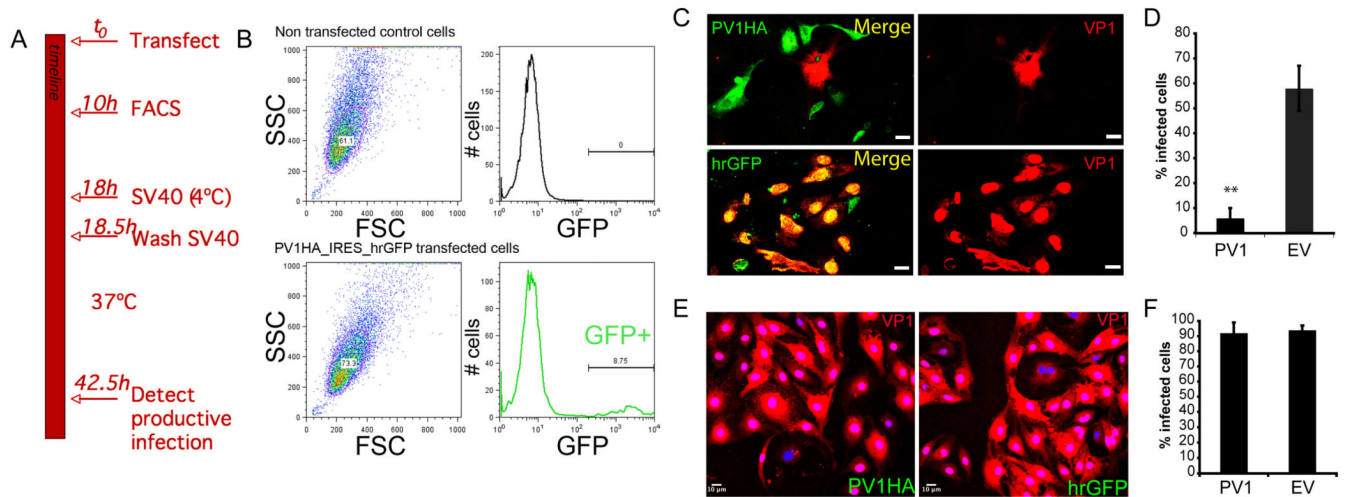


Figure 3. Expression of PV1HA CV-1 cells reduces SV40 infectivity at low but not high viral titers

A) Schematic of the experimental timeline. B) Gating strategy employed for the flow sorting of hrGFP expressing cells to be used for SV40 infection. *Top panels* – non transfected cells. *Bottom panels* – PV1HA-IRES-hrGFP transfected cells. C) Immunofluorescence confocal microscopy demonstrating the reduced SV40 infectivity at low MOI in PV1HA expressing cells (*top panels, PV1HA*), as compared to hrGFP transfected cells (*bottom panels, hrGFP*). Productive infection was detected with anti-VP1 capsid protein antibodies (*red*). hrGFP expressing cells are shown in green. Left panels show both channels (*Merge*) whereas right panels show only VP1 staining (*VP1*). Bars 10 μ m. D) Quantification of the virus producing cells after low titer SV40 infection. The data is expressed as percentage of cells showing VP1 nuclear staining from total cells counted in 10 fields/well at 20 \times magnification (n>200 per well) identified by DAPI staining of nuclei. The columns represent the average of two separate experiments each done in triplicate wells. The error bars represent standard deviation among all replicates. (stdev, n=6 wells, ** p <0.01) E) Immunofluorescence confocal microscopy demonstrating no effect of PV1 on SV40 infectivity at high MOI. Left panel - PV1HA expressing cells (*PV1HA*), right *panel* - control cells (*hrGFP*). Productive infection was detected with anti-VP1 capsid protein antibodies (*red*) whereas DAPI staining of nuclei is shown in blue. Bars 10 μ m. F) Quantification of the virus producing cells after high titer SV40 infection. The data and error bars are as in D) (stdev, n=6 wells, ** p <0.01).

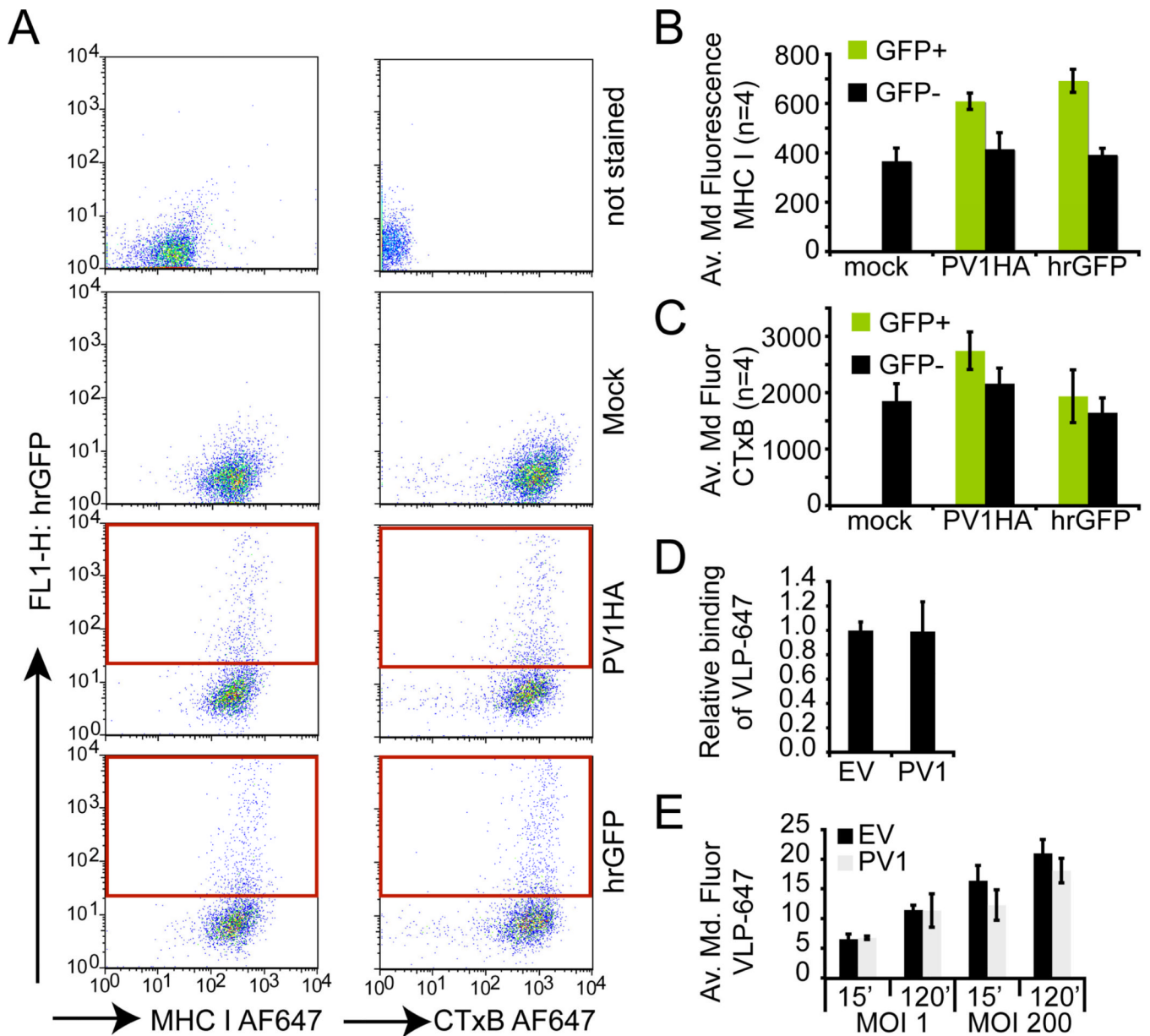


Figure 4. Expression of PV1 does not alter the cell surface expression of SV40 receptors such as GM1 ganglioside and MHC class I molecules

A) Flow cytometry diagrams demonstrating the binding of anti-MHC I-AF647 (*left panels*) and cholera toxin B subunit-AF647 (*CTxB, right panels*). From the top, the panels represent unstained CV-1 cells followed by mock, PV1HA and hrGFP transfected cells. B-C) Average median fluorescence (arbitrary units) of anti-MHC I-AF647 (B) and cholera toxin B subunit-AF647 (C) labeled CV-1 cells that were transfected with no DNA (mock), PV1HA (*PV1HA*) or hrGFP (*hrGFP*). Green columns represent hrGFP positive cells gated as shown in A (*red boxes*). D) Relative binding of VLP-AF647 to hrGFP gated either PV1HA expressing (PV1) or empty vector transfected cells (EV). (n=4, stdev). E) Average median fluorescence documented VLP-AF647 internalization at